Particle-Size-Dependent Distribution of Carboxylate Adsorption Sites on TiO_2 Nanoparticle Surfaces: Insights into the Surface Modification of Nanostructured TiO_2 Electrodes

Qing-Li Zhang,[†] Lu-Chao Du,[†] Yu-Xiang Weng,*[,†] Li Wang,[†] Han-Yuan Chen,[‡] and Jian-Qi Li[‡]

Laboratory of Optical Physics and Beijing Laboratory of Electron Microscopy, Institute of Physics, Chinese Academy of Sciences, Beijing 100080, People's Republic of China

Received: November 25, 2003; In Final Form: July 28, 2004

Size-dependent surface binding forms of the carboxylic group on the surface of TiO_2 nanoparticles were investigated by a surface-binding transient probe molecule all-*trans*-retinoic acid (ATRA), where the excited triplet-state probe molecule generated by a photoinduced interfacial charge recombination for the adsorbed monolayer acts as a reporter for the different surface binding forms. Different TiO_2 nanoparticles of varying size—that is, 6, 0.8−1.4, and 0.7 nm—were prepared, and their physical properties were examined by X-ray diffraction (XRD), transmission electron microscopy (TEM), selected-area electron diffraction (SAED), and X-ray photoelectron spectroscopy (XPS). The transient absorbance difference spectra of the ATRA/TiO_2 reveal that, when the size changes from 6 nm to <1.4 nm, the simple adsorption forms (physical adsorption and hydrogen bonding form) decrease from 36% to 3%, whereas chemical binding forms increase from 74% to 97%. Such a size-dependent effect is attributed to the variation in the relative compositions of surface Ti atoms of different coordination states, which, in turn, form undercoordinated surface defect sites when the size varies at nanoscale. Referring to the results of the size-dependent coordination states of the surface Ti atoms from X-ray absorption near-edge spectroscopy (XANES) [T. Rajh et al., *J. Phys. Chem. B* **1999**, *103*, 3515−3519], the change of relative compositions for the 6-, 5-, and 4-fold coordinated surface Ti atoms, with respect to the particle size, can be rationalized. The dependency of the coordination state of the surface Ti atoms on the particle size provides a quantitative basis for tuning the compositions of the surface Ti atoms of different coordination state, as well as the surface binding forms by the control of the particle size. Surface modifications utilized in the Grätzel cells were discussed, in view of the surface binding and the coordination state of the surface Ti atoms.

Introduction

Wide-gap metal-oxide semiconductor nanoparticles have attracted intense interest, because of their size-dependent photophysical properties.[1−4] It has also been shown that the particle size has a pronounced effect on the chemical activities of the nanoparticles.[5−7] As the size of the crystalline gets down to the nanoscale level, the surface area of the particle increases drastically, and the fraction of the surface atoms also increases inversely proportional to the diameter of the nanoparticles.[8] This results in a substantial amount of surface defects, because of undercoordination of the surface Ti atoms, as well as the surface dangling bonds acting as active sites for the photochemical processes. Thus, by the control of the nanoparticle size and the proper modification of the surface, some of the photophysical and chemical properties of the semiconductor nanoparticles, e.g., the spectral properties of the semiconductors, can be tuned.[9]

Among the various types of metal oxides, titania (TiO_2) is one of the most promising materials in many applications, e.g., quantum dot devices,[10] photocatalysis,[11] and solar energy conversion devices.[12−14] In addition to the proper control of the particle size, effective surface binding is also one of the key steps in the device-orientated application of TiO_2 nanoparticle based on the interfacial photoinduced electron injection.[15−17] In a potentially applicable dye-sensitized mesoporous TiO_2 nanocrystalline solar cell (Grätzel cell),[12] the ruthenium complex dye is attached to the TiO_2 nanoparticle surface through carboxylic groups. As the size of the crystal gets smaller, more facets and surface steps are created, resulting in surface Ti atoms of varied undercoordination states, which, in turn, leads to different physical and chemical surface adsorption forms including the simple adsorption by electrostatic attraction, hydrogen bonding, and chemical binding through the formation of esterlike linkage, bridging, and chelating.[18] These different surface species are expected to have varied electron injection capability. Attempts to correlate the efficiency of the solar energy conversion to the binding form have been reported,[19] and the surface binding forms of carboxylic groups on TiO_2 becomes a subject of intense study.[18,20−25] On the other hand, various surface modification methods have been used to improve the performance of the solar cell, including the treatment of the TiO_2 photoanode with $TiCl_4$ solution prior to sintering of the photoelectrode at the elevated temperature[26] or with hydrochloric acid (HCl) after the sintering of the photoelectrode.[27] Although the aforementioned surface modifications proved to be effective in improving the photoelectric conversion efficiency, the exact mechanisms are still not clear enough.

* Author to whom correspondence should be addressed: Telephone: +86-10-82649342. Fax: +86-10-82649451. E-mail address: yxweng@aphy.iphy.ac.cn.

[†] Laboratory of Optical Physics.

[‡] Beijing Laboratory of Electron Microscopy.

10.1021/jp037584m CCC: $27.50
Published on Web 09/08/2004

SCHEME 1: Schematic Diagram for the Probe Molecule ATRA Forming Three Different Types of Surface Binding at the TiO_2 Surface: (a) Esterlike Linkage, (b) Bridge, (c) Chelating

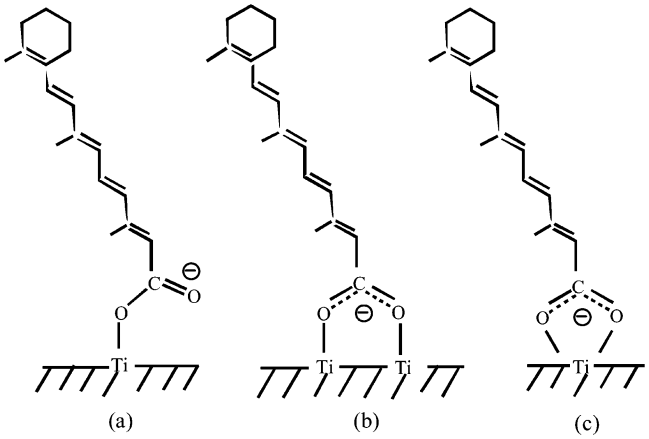

There have been reports of the size effect on the photocatalytic activities,[5−7] the electron diffusion and recombination in the Grätzel cell,[28] and the surface area of the TiO_2 nanoparticles;[29] yet, the size effect on the surface binding forms has not been reported, to the best of the authors' knowledge. Note that there have been studies of size effect on the coordination state of the surface Ti atoms by X-ray absorption near-edge spectroscopy (XANES), which show that, as the size of crystalline TiO_2 decreases from 50 nm down to 2 nm, the coordination state of the surface Ti atoms changes from completely 6-fold coordinated to 5-fold coordinated, providing the first example for the size effect on the coordination state of the TiO_2 surface Ti atom.[30] In our previous study, we have reported a transient molecular-probe method to detect the carboxylic/TiO_2 surface binding forms, which uses the triplet−triplet absorption spectra of the all-*trans*-retinoic acid (ATRA) as an indication for the different types of surface species shown in Scheme 1.[23] In this method, the excited-triplet-state molecule is generated by the interfacial charge recombination between the trapped electron on TiO_2 surface and the cation of the bounded probe molecules, thus the transient probe method is sensitive only to the first adsorption layer. It has been shown that such a transient probe molecule can give a quantitative evaluation of the different adsorption forms of carboxylic groups on the surface of TiO_2.[23]

In this work, we investigated the surface binding forms of the carboxylic groups on the surface of TiO_2 nanoparticles of different size by means of the transient molecular probe, attempting to correlate the surface binding forms and the coordination state of the surface Ti atoms to the size of the nanoparticles. Three different types of TiO_2 nanoparticles of varied sizes were prepared, and their crystallinities were characterized by X-ray diffraction (XRD) and the selected-area electron diffraction (SAED), whereas the valence state of surface Ti atoms were examined by X-ray photoelectron spectra (XPS). Our study clearly shows that the binding forms of carboxylic groups on the surface of TiO_2 nanoparticles are size-dependent, which can be attributed to the change of the coordinate states of the surface Ti atoms, with respect to the change of the particle size. This study also sheds insights onto the understanding of the surface modification of TiO_2 nanoparticle used in the Grätzel cell.

Experimental Section

All-*trans*-retinoic acid (ATRA) (Aldrich), titanium(IV) *n*-butoxide (99%) (ACROS), and titanium(IV) tetra-isopropoxide (ACROS) were used as received. Solvents and other reagents were analytical grade and used without further purification. Three different types of TiO_2 colloidal solutions were prepared by hydrolysis of titanium alkoxides in H_2O, ethanol, and hexanol, respectively. The procedures have been reported elsewhere;[10,26,31] briefly, aqueous TiO_2 colloidal solution was prepared by a dropwise addition of a 50 mL solution of titanium(IV) tetra-isopropoxide dissolved in 20 mL of 2-propanol into 300 mL of deionized H_2O (Milli-Q, Millipore Corp.) containing 1.1 mL of 68% nitric acid cooled by an ice/water bath under vigorous stirring. The resulting turbid mixture was refluxed for 8 h leading to an opaque concentrated TiO_2 colloidal solution. TiO_2 hexanolic and ethanolic colloidal solutions were prepared by hydrolysis of titanium(IV) *n*-butoxide in the acidified hexanol [23] or ethanol at a temperature of 0°C at pH of 3.[32] The clear colloidal solutions were not refluxed at the elevated temperature.

Powdered TiO_2 samples for XRD measurement were prepared by rotary evaporation of the corresponding colloidal solutions at room temperature. The XRD measurements were performed on a D/max-2400 X-ray diffractometer (Rigaku) with Cu Kα radiation. From the line broadening of corresponding XRD peaks, the sizes of nanoparticles were estimated by the Scherrer formula.[33] Samples for transmission electron microscopy (TEM) measurement were typically prepared by allowing the colloidal sample to evaporate on amorphous carbon films. TEM images were recorded on a H-9000 electron microscope (Hitachi). Electron diffraction patterns were acquired on a selected field of particles recorded with a camera length (λ_{CL}) of 1.0 mm-Å. Thin layered samples for XPS analysis were prepared by evaporating a drop of colloidal solution on a clean stainless-steel sheet that was dried in a vacuum desiccator overnight. The measurements were performed on a MKII system (British UG). The X-ray source used for XPS was Mg Kα, and the binding energy (BE) was calibrated using C 1s (BE = 284.6 eV). The flash photolysis setup has been reported elsewhere.[32] Briefly, it used the 355-nm third harmonic generation of the Nd^{3+}:YAG laser as the excitation source (Spectra Physics, LAB 170) with a pulse width (full width at half-measure, fwhm) of 8 ns. The probe beam source was a 500-W continuous wave (cw) xenon lamp, and the transient signal was detected by a six-stage R456 (Hamamatsu) photomultiplier tube, amplified by a 300 MHz dc amplifier (Stanford Research Systems, Inc.), and finally fed into a 500 MHz digital oscilloscope (Tektronix) interfaced to a personal computer (PC) by a general-purpose interface bus (GPIB) board for data handling and processing. During the experiment, the dye-sensitized TiO_2 colloidal solutions were kept bubbling with an argon gas stream. The ATRA-sensitized TiO_2 colloidal alcoholic solution was prepared by an addition of concentrated ATRA methanol solution ($c = 2 \times 10^{-3}$ M) into TiO_2 colloidal solution and stirred for 30 min in darkness under a N_2 stream for dye sensitization, keeping the apparent ATRA concentration in the bulk at 2×10^{-5} M. For ATRA sensitization of aqueous TiO_2 colloid, because of the poor solubility of ATRA in water, the TiO_2 colloid was suspended in methanol prior to the ATRA sensitization; i.e., 1 mL of concentrated aqueous TiO_2 colloid (40 g/L) was diluted to a volume of 20 mL (2 g/L) with 19 mL of methanol. The concentrations of ATRA were similar to those for ATRA/TiO_2 prepared in alcoholic solution. All the ATRA sensitized TiO_2 colloidal solutions were bubbled with high-purity argon gas for at least half an hour to remove the dissolved oxygen.

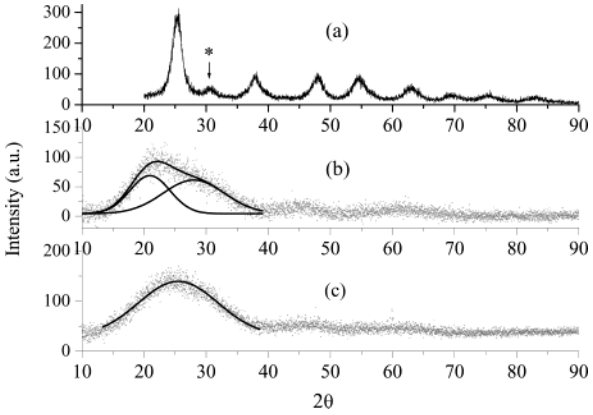

Figure 1. X-ray diffraction (XRD) patterns for the three powdered TiO_2 nanoparticles prepared in (a) water, (b) hexanol, and (c) ethanol.

Results and Discussion

TiO_2 has three polymorphs: rutile, anatase, and brookite. Rutile is the thermodynamic stable phase, whereas anatase is metastable. Solid−solid phase transformation of the anatase phase to the rutile phase has been observed to occur in the temperature range of 500−900 °C.[34,35] Generally, crystalline TiO_2 prepared via the sol−gel method always leads to the anatase phase.

Figure 1 presents the XRD patterns of the powdered TiO_2 samples. The XRD patterns show that the TiO_2 nanoparticles prepared in H_2O consist of mainly anatase, with a small amount of brookite (which matches the brookite (121) face reflection, indicated by an asterisk shown in Figure 1a); this is consistent with the reported results by a similar preparation method.[36,37] The crystallite size estimated from Scherrer formula is 6.0 nm. Comparing the XRD pattern of TiO_2 prepared in ethanol (Figure 1c) to that of TiO_2 prepared in H_2O, the first diffraction peak, which has a Gaussian-type distribution, becomes very smeared and is typical of the amorphous phase. The particle size evaluated from the Scherrer formula is ∼0.7 nm. Although the diffraction pattern of TiO_2 in hexanol becomes asymmetrical and can be resolved into two Gaussian peaks, which indicates that a crystalline phase might have formed in the amorphous phase. Figure 2 displays the SAED patterns of the three different colloidal TiO_2 samples. Figure 2a presents a typical SAED pattern for a polymorphous phase, which shows that the TiO_2 nanoparticles prepared in H_2O are polymorphous. Figure 2c displays a set of diffused rings typical of an amorphous phase, whereas Figure 2b consists of a series of fairly sharp concentric rings, which indicates that TiO_2 prepared in hexanol contains a polycrystalline phase. Combining the results of XRD and SAED, it can be concluded that the TiO_2 prepared in hexanol contains both amorphous and polycrystalline phases. One of the resolved peaks is located at an 2θ angle of 29.6°, similar to that of the brookite (121) face reflection (30.806°), which suggests that brookite can be one of the possible crystalline phases. The particle size estimated by the Scherrer formula is 1.4 nm at the smaller diffraction angle and 0.8 nm at the larger diffraction angle for the two resolved Gaussian peaks. Because the latter is similar to that of an amorphous phase prepared in ethanol, we determined that the size of crystalline TiO_2 prepared in hexanol lies in a range of 0.8−1.4 nm. Figure 3 shows the XPS spectra of the Ti 2p region of the three different TiO_2 samples. The purpose of this experiment is to examine whether the oxidation state of surface Ti atoms are the same for all three samples. The binding energies for the Ti $2P_{3/2}$ and Ti $2p_{1/2}$ core levels are BE = 458.2 and 463.9 eV, respectively, with a BE

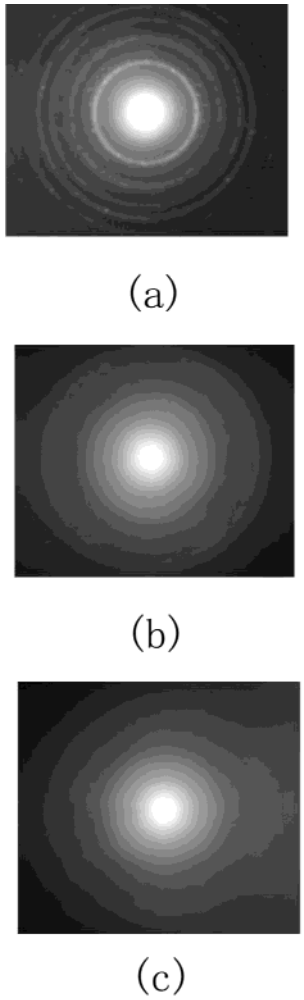

Figure 2. Selected-area electron diffraction (SAED) patterns for the three colloidal TiO_2 nanoparticles prepared in (a) water, (b) hexanol, and (c) ethanol.

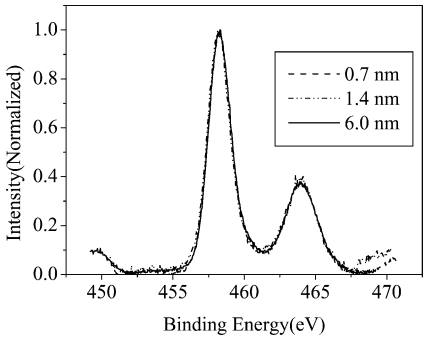

Figure 3. X-ray photoelectron spectroscopy (XPS) spectra of the Ti 2p region of the three different TiO_2 polymorphs with different sizes, prepared in water, hexanol, and ethanol, respectively.

difference of 5.7 eV, which are the typical values for the Ti^{4+} cation.[38−40] Because the shapes of the Ti 2p doublet are virtually the same for all three samples, it is concluded that the oxidation state of the surface Ti atoms for the three samples is Ti^{4+}.

Figure 4 displays the transient absorbance difference spectra of the probe molecule adsorbed on the three different colloidal TiO_2 nanoparticles of varied size. These absorption signals have been confirmed to be derived from the triplet−triplet absorption of the different ATRA surface binding species generated in a photoinduced interfacial charge recombination process.[23,32] The dotted line in Figure 4 is the reference triplet−triplet absorption

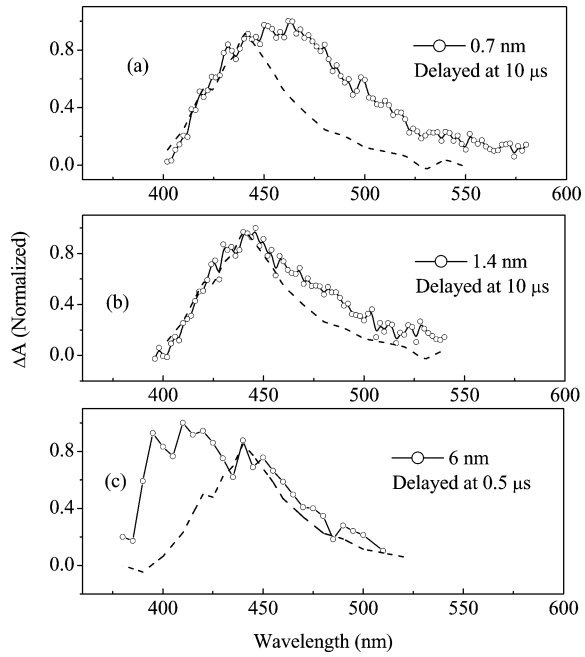

Figure 4. Transient absorbance difference spectra for TiO_2 colloidal solutions of three different sizes, sensitized by the ATRA probe molecules (TiO_2 prepared in (a) ethanol, (b) hexanol, and (c) water). The transient absorbance difference spectra were acquired by excitation at 355 nm, 1 μJ/pulse. The reference transient absorbance spectrum in the three panels is the triplet−triplet absorption spectrum of the esterlike model compound tri-butoxyl titanium(IV) all-*trans*-retinoate.[23]

spectrum of a model compound with an esterlike linkage between titanium(IV) and all-*trans*-retinoate (tri-butoxyl titanium(IV) all-*trans*-retinoate), which has a peak triplet−triplet absorption at 440 nm.[23] We have shown in our previous work that, when exciting the ATRA/TiO_2 colloidal solution, photoinduced electron injection from ATRA to the TiO_2 nanoparticle occurs, followed by a charge recombination between the trapped electron on TiO_2 surface and the ATRA cation forming the excited triplet-state ATRA molecule with a substantial yield.[23,32,41] The interfacial-charge-recombination-generated excited triplet-state molecule has a triplet−triplet absorption spectrum that is typical of the binding forms, e.g., the simple adsorption form (physical adsorption by electrostatic attraction and hydrogen bonding) of the ATRA anion on the TiO_2 surface has a triplet−triplet adsorption peak at 419 nm, that of the esterlike linkage form appearing at 440 nm, the bridge form at 450 nm, and chelating form at 465 nm or longer wavelengths.[23] When using the triplet−triplet absorption spectrum of the model compound as the reference spectrum shown in Figure 4, the simple adsorption forms would simply appear in the blue side of the spectral region, with respect to the reference spectrum, whereas that of the bridge and chelating forms emerge in the red side.

Figure 4 shows a clear tendency that the transient difference absorption spectra of ATRA/TiO_2 shift to the red side as the size and crystallinity of the TiO_2 nanoparticles decrease. Assuming that the molar absorption coefficients of the different surface binding forms are similar, the compositions of the different surface adsorption forms (simple adsorption, esterlike linkage, bridge plus chelating), on the basis of their integrated intensities, of the triplet−triplet absorption spectra are listed in Table 1. This table shows that, when the crystallinity of TiO_2 changes from polycrystalline, with an average size of 6 nm, to an X-ray amorphous form 0.7 nm in size, the proportion of simple adsorption form decreases from 36% to 3%, whereas that of the chelating form increases from almost 0% to 44% (the deduction of the individual constitution of bridge and chelating forms will be given later). Apparently, the results also indicate that a remarkable change of the surface state of the TiO_2 nanoparticles occurs when the TiO_2 nanoparticle changes from a crystalline phase to an X-ray amorphous phase, which is caused most probably by the change in the coordination state of the surface Ti atoms.

For the anatase, the building block is a slightly distorted TiO_6 octahedron. In the bulk, the Ti atom is 6-fold coordinated and the O atom is 3-fold coordinated. At the surface, the crystals are truncated along some stable laminal planes. For anatase, the (101) and (001) planes are the dominant planes, either in the synthesized nanocrystal or naturally occurring minerals.[37,38,42] Two types of surface terminations, shown in Figure 5, are generally used to create a (001) crystal plane,[38] thus creating 6-fold and 5-fold coordinated surface Ti atoms, respectively, whereas, along the edges or at the corner, the Ti atoms are 4-fold coordinated (these are known as "corner defects").[30] Therefore, the surface Ti atoms exist mainly in three forms, i.e., 6-fold, 5-fold, and 4-fold coordinated. The relative ratio of these three types of surface atoms are expected to be dependent on the particle size. In a recent study of the surface Ti atoms with XANES at varying TiO_2 crystalline sizes, it has been shown that the coordination of surface Ti atoms changes from 6-fold in 50.0-nm particles to 5-fold in 2-nm particles.[30] Because 5-fold and 4-fold coordinated Ti atoms are undercoordinated, they are expected to be chemically more active than the 6-fold coordinated surface Ti atoms, in regard to the surface binding. Therefore, the 6-fold coordinated Ti atoms are expected to have a tendency to act as sites for simple adsorption, whereas the undercoordinated Ti atoms act as sites for chemical binding. In addition, the 5-fold coordinated Ti atoms would favor to form an esterlike linkage and a bridging bond, whereas 4-fold coordinated atoms are inclined to form a chelating bond with the carboxylic groups, based on their unsaturated coordination number. Table 1 shows that the simple adsorption form occupies 35% of the total adsorbed forms for 6-nm polycrystalline TiO_2, whereas this value decreases to ~3% for polycrystalline TiO_2 0.8−1.4 nm in size and amorphous TiO_2 0.7 nm in size. This fact suggests that, even for a TiO_2 surface with totally undercoordinated Ti atoms (amorphous TiO_2), ~3% of the surface atoms still exist as sites for simple adsorption, which is possibly realized by the formation of hydrogen bonding between the carboxylic groups and the surface hydroxyl groups. After a correction for the contribution from the undercoordinated surface Ti atoms to the simple adsorption forms, the simple adsorption on the 6-fold coordinated surface Ti atoms constitute ~33% of the composition for 6-nm polycrystals. This roughly corresponds

TABLE 1: Size-Dependent Surface Adsorption Forms of Carboxylic/TiO_2 Nanoparticles Revealed by the Transient Molecular Probe

medium in which TiO_2 is prepared	crystallinity	Adsorption Form				
		simple adsorption	ester-like	chelating+bridge	bridge	chelating
H_2O	polycrystal	36%	57%	7%	7%	0%
hexanol	polycrystal/amorphous	3%	68%	30%	9%	21%
ethanol	amorphous	3%	47%	50%	6%	44%

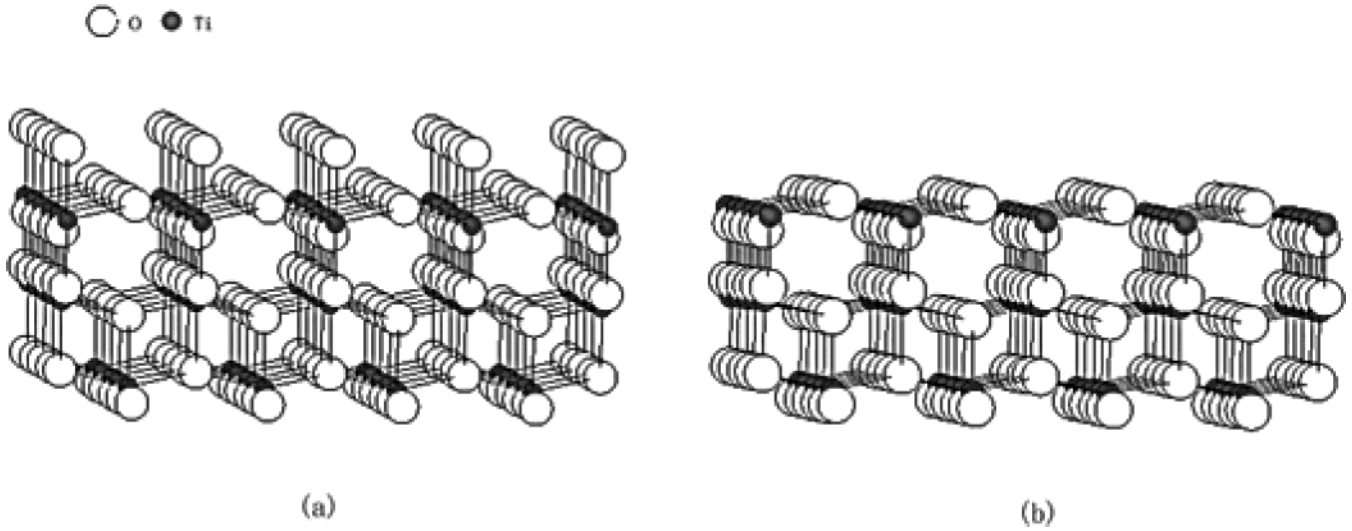

Figure 5. Two surface terminations used to generate a model of (a) a 6-fold coordinated titanium surface and (b) a 5-fold coordinated titanium surface in a frame of an anatase crystal structure.

TABLE 2: Compositions of the Three Different Surface Ti Atoms with Various Sizes

		composition (%)		
sample	size (nm)	6-fold	5-fold	4-fold
single crystal[a]	50	100	0	0
polycrystalline	6	33	67	0
nanoparticle[a]	2	0	100	0
polycrystalline/amorphous	1.4	0	79	21
amorphous(<1 nm)	0.7	0	57	43
$Ti_{16}O_{32}$[b]	1.2[c]	0	37.5	62.5

[a] Results from XANES experiment.[30] [b] Theoretical prediction from the smallest possible TiO_2 crystallite.[44] [c] The effective diameter was obtained by converting the volume of the structural unit of $Ti_{16}O_{32}$ into a sphere.

to the fact that approximately one-third of the surface Ti atoms are 6-fold coordinated for a 6-nm TiO_2 polycrystalline sample, whereas the remaining surface Ti atoms are mainly 5-fold coordinated. The composition of 5-fold coordinated surface Ti atoms for the 6-nm TiO_2 nanoparticle (67%) falls between that for 2-nm TiO_2 nanocrystals (100%) and 50-nm TiO_2 nanocrystals (0%), as determined by XANES (see Table 2), which is consistent with the tendency predicted by the XANES measurement. From Table 1, two clear tendencies can be observed; that is, as the TiO_2 nanoparticle changes from the polycrystalline form to the amorphous phase, the simple adsorption form decrease by 10-fold, while the chelating together with bridge form increase by 7-fold in magnitude, which reflects the size-dependent change of relative compositions of the three different types of surface Ti atoms. Based on the triplet−triplet absorption spectrum and the coordination state of the surface Ti atoms from the XANES experiment, it is concluded that the composition of the 4-fold coordinated Ti atoms can be very small in 6-nm TiO_2 nanoparticles; therefore, we have determined that the 7% portion initially attributed to the summed contribution of the bridge and chelating forms solely comes from the bridge form in 6-nm TiO_2 nanoparticles. For the 5-fold coordinated surface Ti atoms, they can form either an esterlike or a bridged linkage with the carboxylic groups, and we assume that the ratio for the formation of esterlike linkage and the bridge form in 6-nm TiO_2 nanoparticles (7%/57% = 12%) holds for the other two samples, with a smaller size of 0.8−1.4 and 0.7 nm, respectively. Thus, the individual compositions of the bridge and chelating form of ATRA binding on TiO_2 nanoparticles can be resolved, as listed in Table 1. Table 2 summarizes the size effect of TiO_2 nanoparticles on the compositions of the surface Ti atoms of different coordination numbers by the transient molecular-probe method. The results of the XANES experiment are also included. Interestingly, note that the smallest anatase nanocrystal predicted in a theoretical work is $Ti_{16}O_{32}$ with an estimated effective diameter of 1.2 nm.[44] The calculated compositions of the 5-fold and 4-fold surface Ti atoms for this smallest nanocrystal are 37.5% and 62.5%, respectively. The counting of the surface Ti atoms and the evaluation of the size for the structural unit $Ti_{16}O_{32}$ were accomplished with home-written software. This theoretical result is also listed in Table 2.

Our results show that the binding forms of carboxylic groups on the TiO_2 nanoparticle surface are dependent on the size of the particles. For particle sizes of <6 nm, the esterlike linkage is always the dominant surface species. When the size increases, the fraction of the simple adsorption form is also expected to increase. For 50-nm TiO_2 nanoparticles, most of the adsorbed forms would be expected to be the simple adsorption form. In contrast, when the particle size is reduced to <2 nm, 97% of the surface binding forms would be chemical binding forms of esterlike linkage, bridge, and chelating forms. In addition, the relative compositions of the three different types of surface Ti atoms are varied to the size of the nanoparticles, i.e., the surface adsorption forms can be controlled by adjusting the particle size. We also found that the surface binding of ATRA onto the TiO_2 surface is critical to the pH value of the colloidal solution. At pH >3.9, no observable transient absorption signal can be found in the three different ATRA/TiO_2. At a higher pH value, the ATRA molecule exists mainly as the retinoate anion form. This indicates that the retinoate anion may not adsorb to the TiO_2 effectively at pH >3.9.

The conclusion that the major surface binding form for carboxylic group on TiO_2 surface is the esterlike linkage form seems inconsistent with that from several investigations on monocarboxylic and multicarboxylic acids adsorbed on TiO_2 film by attenuated total reflectance infrared (ATR−IR) spectroscopic study. It has been shown that IR spectroscopy can be used for the investigation of different adsorption forms of carboxylic acid on a TiO_2 surface, that is, unidentate chelating, bidentate chelating, and bridging coordination with surface Ti atoms, although the conclusions among different authors are controversial, in regard to the assignment of the major binding

forms.[18−20] The discrepancy in the assignment mainly results from the different experimental conditions, such as pH and the concentration used in different groups. For example, IR spectroscopic study of multicarboxylic adsorbates is complicated by the pH of the sample. The pH value not only affects the surface adsorption form, but also its uncoordinated carboxylic group. At a lower pH that is favorable to form chemical binding, it is difficult to identify whether the IR absorption peak at ~1700 cm^{-1} is resulting from the esterlike linkage binding form or the free distal carboxylic group, whereas at a higher pH value, the distal carboxylic acid group becomes carboxylate; however, this condition may not favor chemical binding at the surface. For monocarboxylic acid, a similar situation might occur with the assignment of a binding form at the interface or the nonbinding forms near the surface. Another uncertainty may result from the concentration effect. Because the effective optical path length for ATR−IR can be as long as several hundred nanometers,[45] if the concentration of the adsorbate is not controlled intentionally, the ATR−IR signal may include the multilayer contribution, which suggests that the IR signal may not accurately report the information of the adsorbed single layer. On the other hand, it has been reported that the multilayer adsorption can even change the adsorption form of the first layer, as observed in the case of glutamic acid adsorbed on a TiO_2 surface,[46] where, at an adsorbate concentration similar to or less than that required for the monolayered adsorption ($c = 5 \times 10^{-6}$ M), the observed IR absorption intensity for the esterlike linkage form (1683 cm^{-1}) has approximately the same intensity as that of the carboxylate form (1523 cm^{-1}) at pH 3.0; however, at a higher concentration (e.g., $c = 5 \times 10^{-4}$ M), the IR absorption intensity for the esterlike linkage form becomes almost indiscernible. Interestingly, in a recent surface-enhanced infrared absorption spectroscopy (SEIRAS) experiment, which is sensitive only to the adsorbed monolayer, the experiment shows that acetic acid adsorbed on the TiO_2 surface, with a major absorption peak at 1715 cm^{-1} that is attributable to the esterlike linkage form.[47] Therefore, our result is consistent with those of IR studies reflecting the adsorption monolayer at a proper pH and concentration. Our effort of Fourier transform infrared (FT-IR) spectroscopic study of ATRA adsorbed on TiO_2 either in colloidal solution or on TiO_2 film only show a certain indication that ATRA can be bonded to the surface Ti atoms through esterlike linkage. In the experiment, we used D_2O instead of H_2O during the preparation of TiO_2 nanoparticles. The TiO_2 film for IR measurement was prepared via the vacuum evaporation of drops of a TiO_2−ethanol colloidal solution on a CaF_2 substrate; whereas the ATRA-sensitized TiO_2 film was prepared via the vacuum evaporation of the ATRA ($c = 2 \times 10^{-4}$ M) sensitized TiO_2 colloidal solution (2 g/L). The IR absorption spectrum of either the colloid or the film showed a broad and intense absorption band, ranging from 1600 to 1700 cm^{-1}, derived from the adsorbed D_2O/H_2O on the TiO_2 surface, strongly interfering with the observation of the esterlike linkage binding form expected in this region. On the other hand, the intense IR absorption peak at 1425 cm^{-1} from the polyene backbone and those from 2-propanol, which is produced during the hydrolysis, would also interfere with the detection of the vibration modes of the carboxylate anion. Therefore, it is difficult to characterize the distribution of the different ATRA surface binding forms. We observed absorption peaks at ~1700 cm^{-1} in both ATRA-sensitized TiO_2 film and ATRA/TiO_2 ethanol solution, which can be attributed to the esterlike linkage binding form; however, uncertainty may still arise, because of the limitations mentioned previously.

Finally, with the knowledge of the compositions of the differently coordinated surface Ti atoms at various particle sizes, some of the surface modification procedures used in improving the performance of the Grätzel cell can be understood, in view of size-dependent surface binding of the carboxylic groups.

1. Surface Modification with $TiCl_4$. Treatment of the photoanode with $TiCl_4$ solution prior to the sintering of the photoanode at the elevated temperature has proven to be an effective approach to improve the performance of the solar cell. In the previous report, it is believed that the $TiCl_4$ treatment covers the relatively impure core (Degussa P25, containing 100 ppm Fe_2O_3) with a thin layer of high-purity TiO_2.[26] Although the real mechanism can be more complicated, conversion of the simple adsorption sites to chemical adsorption sites by such a treatment could be one of the possible causes. Because P25 has an average size of 25 nm, which is estimated to have at least 60% of the 6-fold coordinated surface Ti atoms, based on an assumption that a linear relation holds for the size-dependent composition of 6-fold coordinated surface Ti atoms in a range of 6−50 nm. In terms of the coordination state of the surface Ti atoms, only <40% of the surface Ti atoms are available as chemical adsorption sites for a 25-nm particle. Treatment of $TiCl_4$ via controlled hydrolysis is expected to create much-smaller crystallites on a larger surface of the P25 nanocrystal. In addition to an increase of the surface area, the undercoordinated surface Ti atoms would increase dramatically, which can lead to a substantial increase in the chemical adsorption surface sites, compared to that which is untreated. We believe that it is the change of the surface state that has an important role in improving the performance of the solar cell.

2. Surface Modification with Acid. An increase of the photocurrent for a certain adsorbed organic dye as high as 329% and a photon-to-electron conversion efficiency of 260%, after treatment of the photoanode with HCl have been reported.[24] An immediate expected effect of such a surface treatment can be an increase in the surface area, because of the acid erosion of the particle, but the improvement of the solar cell cannot be explained solely by the increase of the surface area:[24] newly created surface active sites, which are directly related to the surface binding forms, are very probable causes. Treatment with acid would cause acidic etching of the crystal surface, and this etching is most probably nonselective for the crystal plane, which would create more surface steps and an edge on the surface of the crystal. Surface etching not only increases the surface area, but also increases the fraction of the undercoordinated surface Ti atoms, hence providing the chemical adsorption sites for bidentate binding, as observed for sulfonic[48] and phosphate[49] adsorption on TiO_2 via IR spectroscopy. Such an effect would be effective in converting the simple adsorption forms to the chemical adsorption forms, thus leading to the improvement of the photon-to-electron conversion efficiency.

3. Formation and Degradation of the Surface Chemical Bonding. Murakoshi et al. reported that, when refluxing the RuN3-adsorbed Degussa P25 film and nanocrystalline TiO_2 film in ethanol solution,[19] a promotion in the formation of ester binding was observed, which was accompanied by an increase in the photon-to-electron conversion efficiency. As we have shown, when the size of a TiO_2 nanoparticle exceeds 2 nm, some surface sites always exist for simple adsorption, depending on the size of the particles. Reflux in ethanol at an elevated temperature under acidic conditions is expected to favor esterification of the simple adsorption form, existing as hydrogen bonding by depletion of a water molecule, converting the simple adsorption form to the chemical adsorption form. Therefore,

an increase in the photon-to-electron conversion efficiency is expected. On the other hand, one of the important procedures in constructing the Grätzel cell is to use anhydrous media. In view of surface chemical bonding, water at least has two hazardous effects on the surface binding forms: (i) water can coordinate to the undercoordinated surface Ti to form a surface hydroxyl group, and these surface hydroxyl groups convert the chemical adsorption sites to simple adsorption sites via the formation of hydrogen bonding; and (ii) the esterlike linkage is expected to be vulnerable to the hydrolysis reaction, leading to a less-effective surface binding and long-term instability. As a conclusion, any effective surface modification should lead to an increase in the fraction and stability of the surface chemical binding.

Conclusions

Titania (TiO_2) nanoparticles of three different sizes—0.7 nm (amorphous), 0.8−1.4 nm (polycrystal-like), and 6.0 nm (polycrystal)—were prepared via the hydrolysis of titanium alkoxide in different media. Their crystallinities have been examined by X-ray diffractometry and selected-area electron diffractometry, and the sizes were evaluated using the Scherrer formula. The oxidation state of the surface Ti atoms, as determined by X-ray photoelectron spectroscopy, for the three samples are all Ti^{4+}. Surface binding forms have been investigated using the transient molecular probe method, which reveals that the surface binding forms are size-dependent. As the size of the nanoparticle gets smaller, the composition of the simple adsorption forms decreases, whereas that of the chemical adsorption forms increases. These are caused by the size-dependent change of coordination number of the surface Ti atoms, providing a quantitative basis for the size control of the surface binding forms. This gives a new account of surface modifications used in the Grätzel cell.

Acknowledgment. We thank Dr. Q.-L. Guo for his help in XPS measurement, and Prof. D. S. Wang for the home-written software used to generate the TiO_2 crystal structural models and count the surface atoms. This work is supported by the National "Hundreds Talent Program" and National Fund for Key Basic Research, under Grant No. G1998010102.

References and Notes

(1) Alivisatos, A. P. *Science* **1996**, *271*, 933.
(2) Brus, L. *Appl. Phys. A* **1991**, *A53*, 465.
(3) Henglein, A. *Chem. Rev.* **1989**, *89*, 1861.
(4) Micic, O. I.; Nozik, A. J. *J. Lumin.* **1996**, *70*, 95.
(5) Ohtani, B.; Handa, J.-I.; Nishimoto, S.-I.; Kagiya, T. *Chem. Phys. Lett.* **1985**, *102*, 292.
(6) Sclafani, A.; Palmisano, L.; Schiavello, M. *J. Phys. Chem.* **1990**, *94*, 829.
(7) Tanaka, K.; Capule, M. F.; Hisanaga, T. *Chem. Phys. Lett.* **1991**, *187*, 73.
(8) Chen, L. X.; Rajh, T.; Wang, Z.; Thurnauer, M. C. *J. Phys. Chem. B* **1997**, *101*, 10688−10697.
(9) Serpone, N.; Lawless, D.; Khairutdinov, R. *J. Phys. Chem.* **1995**, *99*, 16646−16654.
(10) Colvin, V. L.; Schlamp, M. C.; Alivisatos, A. P. *Nature* **1994**, *370*, 354−357.
(11) Linsebigler, A. L.; Lu, G.; Yates, J. T., Jr. *Chem. Rev.* **1995**, *95*, 735−758.
(12) O'Regan, B.; Grätzel, M. *Nature* **1991**, *353*, 737−739.
(13) Hagfeldt, A.; Grätzel, M. *Chem. Rev.* **1995**, *95*, 49−68.
(14) Moser, J. E.; Bonnote, P.; Grätzel, M. *Coord. Chem. Rev.* **1998**, *171*, 245−250.
(15) Ellingson, R. J.; Asbury, J. B.; Ferrere, S.; Ghosh, H. N.; Sprague, J. R.; Lian, T.; Nozik, A. J. *J. Phys. Chem. B* **1998**, *102*, 6455−6458.
(16) Asbury, J. B.; Hao, E.; Wang, Y.; Ghosh, H. N.; Lian, T. *J. Phys. Chem. B* **2001**, *105*, 4545−4557.
(17) Benkö, G.; Kallioinen, J.; Korppi-Tommola, J. E. I.; Yartsev, A. P.; Sundström, V. *J. Am. Chem. Soc.* **2002**, *124*, 489−493.
(18) Meyer, T. J.; Meyer, G. J.; Pfennig, B. W.; Schoonover, J. R.; Timpson, C. J.; Wall, J. F.; Kobusch, C.; Chen, X.; Peck, B. M.; Wall, C. G.; Ou, W.; Erickson, B. W.; Bignozzi, C. A. *Inorg. Chem.* **1994**, *33*, 3952−3964.
(19) Murakoshi, K.; Kano, G.; Wada, Y.; Yanagida, S.; Miyazaki, H.; Matsumoto, M.; Murasawa, S. *J. Electroanal. Chem.* **1995**, *396*, 27−34.
(20) Finnie, K. S.; Bartlett, J. R.; Woolfrey, J. L. *Langmuir* **1998**, *14*, 2744.
(21) Shklover, V.; Ovchinnikov, Y. E.; Braginsky, L. S.; Zakeeruddin, S. M.; Grätzel, M. *Chem. Mater.* **1998**, *10*, 2533−2541.
(22) Duffy, N. W.; Dobson, K. D.; Gordon, K. C.; Robinson, B. H.; McQuillan, A. J. *Chem. Phys. Lett.* **1997**, *266*, 451−455.
(23) Weng, Y. X.; Li, L.; Liu, Y.; Wang, Li.; Yang, G.-Z. *J. Phys. Chem. B* **2003**, *107*, 4356−4363.
(24) Nazeeruddin, M. K.; Humphry-Baker, R.; Liska, P.; Grätzel, M. *J. Phys. Chem. B* **2003**, *107*, 8981−8987.
(25) Dobson, K. D.; McQuillan, A. *J. Spectrochim. Acta Part A* **1999**, *55*, 1395−1405.
(26) Nazeeruddin, M. K.; Kay, A.; Rodicio, I.; Humphry-Baker, R.; Müller, E.; Liska, P.; Vlachopoulos, N.; Grätzel, M. *J. Am. Chem. Soc.* **1993**, *115*, 6382−6390.
(27) Wang, Z.-S.; Li, F.-Y.; Huang, C.-H. *J. Phys. Chem. B* **2001**, *105*, 9210−9217.
(28) Nakade, S.; Saito, Y.; Kubo, W.; Kitamura, T.; Wada, Y.; Yanagida, S. *J. Phys. Chem. B* **2003**, *107*, 8607−8611.
(29) Ohtani, B.; Zhang, S.-W.; Nishimoto, S.-I.; Kagiya, T. *J. Photochem. Photobiol., A* **1992**, *64*, 223.
(30) Rajh, T.; Nedeljkovic, J. M.; Chen, L. X.; Poluektov, O.; Thurnauer, M. C. *J. Phys. Chem. B* **1999**, *103*, 3515−3519.
(31) O'Regan, B.; Moser, J.; Anderson, M.; Grätzel, M. *J. Phys. Chem.* **1990**, *94*, 8720.
(32) Weng, Y. X.; Li, L.; Liu, Y.; Wang, L.; Yang, G. Z.; Sheng, J. Q. *Chem. Phys. Lett.* **2002**, *355*, 294−300.
(33) Klug, H.; Alexander, L. E. *X-ray Diffraction Procedure*, 2nd Ed.; Wiley; New York, 1974; p 618.
(34) Hague, D. C.; Mayo, M. J. *J. Am. Ceram. Soc.* **1994**, *77*, 1957−1960.
(35) Kumar, K. P.; Burggraaf, A. J.; Okubo, T.; Nagamoto, H. *J. Mater. Chem.* **1993**, *3*, 1151−1159.
(36) Kim, S.-J.; Park, S. D.; Jeong, Y. H.; Park, S. *J. Am. Ceram. Soc.* **1999**, *82*, 927−932.
(37) Zaban, A.; Aruna, S. T.; Tirosh, S.; Gregg, B. A.; Mastai, Y. *J. Phys. Chem. B* **2000**, *104*, 4130−4133.
(38) Burnside, S. D.; Shklover, V.; Barbé, C.; Comte, P.; Arendse, F.; Brooks, K.; Grätzel, M. *Chem. Mater.* **1998**, *10*, 2419−2425.
(39) Silversmit, G.; Poelman, H.; Fiermans, De Gryse, R. *Solid State Commun.* **2001**, *119*, 101−104.
(40) Guo, Q.; Oh, W. S.; Goodman, D. W. *Surf. Sci.* **1999**, *437*, 49−60.
(41) Zubavichus, Y. V.; Slovokhotov, Y. L.; Nazeeruddin, M. K.; Zakeerudin, S. M.; Grätzel, M.; Shklover, V. *Chem. Mater.* **2002**, *14*, 3556−3563.
(42) Zhang, L.; Yang, J.; Quan, D.-H.; Wang, L.; Yang, G.-Z.; Weng, Y.-X. *J. Phys. Chem. B* **2003**, *107*, 13688−13697.
(43) Hengerer, R.; Bolliger, B.; Erbudak, M.; Grätzel, M. *Surf. Sci.* **2000**, *460*, 162−169.
(44) Persson, P.; Gebhardt, J. C. M.; Lunnell, S. *J. Phys. Chem. B* **2003**, *107*, 3336−3339.
(45) Dobson, K. D.; Connor, P. A.; McQuillan, A. J. *Langmuir* **1997**, *13*, 2614−2616.
(46) Roddick-Lanzilotta, A. D.; McQuillan, A. J. *J. Colloid Interface Sci.* **2000**, *227*, 48−54.
(47) Sato, S.; Ueda, K.; Kawasaki, Y.; Nakamura, R. *J. Phys. Chem. B* **2002**, *106*, 9054−9058.
(48) Bandara, J.; Mielczarski, J. A.; Kiwi, J. *Langmuir* **1999**, *15*, 7670−7679.
(49) Connor, P. A.; McQuillan, A. J. *Langmuir* **1999**, *15*, 2916−2921.